A sedimentological approach for classifying sub-surface mine wastes: implications for shallow mine geothermal energy.

Billy J. Andrews[1*], Zoë A. Cumberpatch[2], Zoe K. Shipton[1], Richard Lord[1]

1) Department of Civil and Environmental Engineering, University of Strathclyde, Glasgow, G11XJ.
2) Department of Earth and Environmental Sciences, University of Manchester, Manchester, M13 9QQ.

Correspondence to: Billy J. Andrews (billy.andrews@strath.ac.uk)

Abstract. Following sub-surface coal extraction, workings become flooded and represent a potential aquifer for shallow geothermal development projects. We investigate the internal structure of collapsed mine workings in surface exposures of pillar and stall mine workings exposed through coastal erosion at Whitley Bay, NE England, UK. These workings collapsed in stages, leaving a clay-rich anthropogenic sedimentary layer consisting of collapse breccias and muds that gradually reduce the permeability of the system. Our data suggests workings do not collapse as individual events and that sections near pillars may remain open to flow for years after the rest of the workings have collapsed.

1. Introduction

The importance of coal during the industrial revolution and the large workforce required for its sub-surface extraction led to the development of densely populated areas underlain by a labyrinth of mine workings. Following the decline of sub-surface extraction, groundwater returns to pre-mining levels flooding the mine workings (Younger, 2002). These workings provide potentially large aquifers (e.g. $5.1 \times 10^{12} L$ (Watzlaf and Ackman, 2006)) that can be tapped to extract inexpensive low-enthalpy geothermal heat using ground source heat pumps (Dochartaigh, 2009; Malolepszy et al., 2005; Monaghan et al., 2017). Additionally aquifers can be 'charged' with waste heat created through industry (e.g., refrigeration) and later extracted when required (i.e. the winter) (Hamm and Sabet, 2010; Patsa et al., 2015; Sanner, 2001). Geothermal energy, in particular ground source heat pumps tapping flooded mine waters, have significant potential in the decarbonisation and regeneration of densely populated ex-coal mining areas (Malolepszy et al., 2003; 2005; Hamm and Sabet, 2010).

Open loop systems are typically employed for minewater geothermal systems, with coupled extraction and injection wells (Banks et al., 2019). For production to be sustained, groundwater flow between the injection and extraction boreholes is required, ideally with void space or permeable collapse material intersected by both boreholes, while the water capacity of the mine should be high (Loredo et al., 2016; Lund, 2001). The water capacity, defined here as the volume of water which can be extracted from the mine or mine reservoir (Loredo et al., 2017; Menéndez et al., 2019) can reduce the effective volume and permeability of this void. While the methods of coal extraction varied through time (e.g. bell pits), the pillar and stall method was widely used (Fig. 1) (Bell and Bryn, 1999). Using this method coal was extracted from 'stalls', or 'rooms', supported by pit-props (Daunton, 1981) and pillars wherein, 30 to 70% of the coal remained unworked to support the roof (Fig. 1) (Garrard and Taylor, 1988; Wardell and Wood, 1965). For mine geothermal prospects, the majority of flow will occur through open stalls, which will have a near infinite permeability (Loredo et al., 2017).

Rock pillars and temporary supports (e.g. pit props, colliery arches) are designed to sustain the weight of the overburden, however, following mining operations local stresses, rotting timbers, and the spalling of the pillars, can cause the roof to fail and eventually collapse (Bruyn and Bell, 1999; Helm et al., 2013; Lokhande et al., 2005). The failure of a single pillar will cause other pillars, particularly those in an up-dip direction, to become increasingly stressed and risk collapse causing a knock-on effect until the support of the overburden is significantly reduced (Bruyn and Bell, 1999). As roof material falls, the stalls become clogged and deformation migrates upwards in a predictable manner (e.g. Garrard & Taylor 1988; Madden and Hardmam, 1992), eventually forming crown holes at the surface. Pillar collapse and roof spalling, which can occur many years after mining operations have ceased (Carter *et al.* 1981; Salmi *et al.* 2019a, b) can lead to widespread subsidence (Gee et al., 2017) often occurring as individual events over relatively short time scales (days to weeks) (Carter et al., 1981; Marino and Gamble, 1986).

While the structure above the collapsed workings has been studied by many authors (e.g. Garrard and Taylor, 1988; Helm et al., 2013), the lithologies which make up the collapsed section and the processes by which they are deposited has received little attention. With the emergence of shallow mine geothermal projects it is now important to understand the characteristics of these ‘mine wastes’, and the processes involved if we are to improve our estimations of the water capacity of pillar and stall workings for geothermal energy. To address this we investigate exposures of workings at Whitley Bay exhumed by costal erosion using a detailed sedimentological approach and highlight the implications of our findings for shallow mine geothermal projects targeting pillar and stall workings. We find that the net water capacity and permeability of a potential mine geothermal site degrades progressively after abandonment as the roof spalls, and finally collapses.

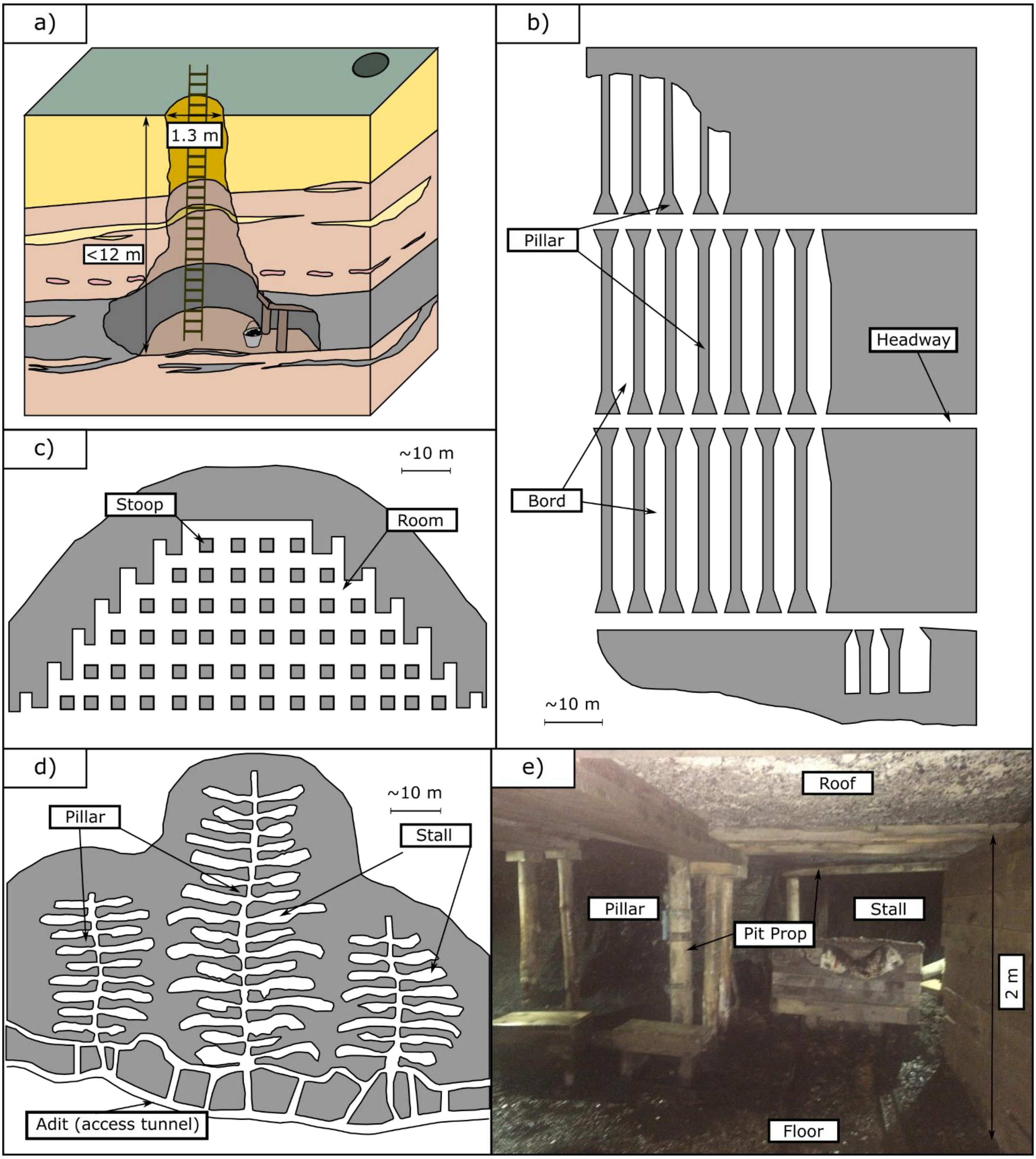

Figure 1: Typical UK shallow mining methods. (b) to (d) show variations on the pillar and stall mining methods with regional variations in terminology and layout. (b, c and d redrawn from Bruyn and Bell (1999) a) bell pit, b) Bord-and-pillar workings, Newcastle upon Tyne (17th Century), c) Stoop and room workings, Scotland (17th Century), d) Pillar and stall workings, South Wales (17th Century), e) Photograph of pillar and stall workings, Beamish open air museum.

2. Geological history

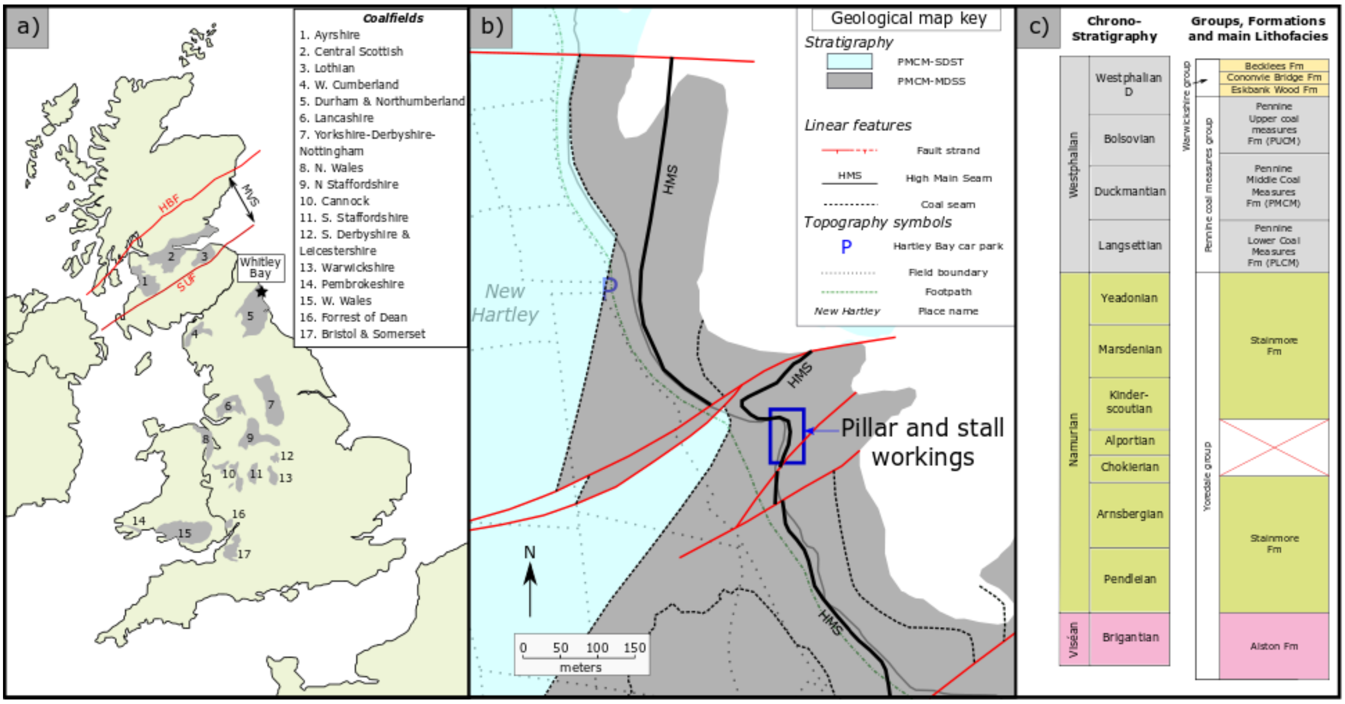

Figure 2: Geological setting. a) location of field site and UK coal fields (after (Donnelly et al., 2008), b) geology surrounding the workings at Whitley Bay, Northumberland (The map is modified from Geological Map Data BGS©UKRI (2018)) PMCM-SDST, c) Chrono-stratigraphy, formations and lithofacies of the Northumberland Trough (Chadwick et al., 1995). SDST = stand stone dominant sequence, MDSS = mudstone dominant sequence.

UK Coal mines are found within numerous late-Devonian to early Carboniferous, east-west trending basins (Fig. 2a) that formed in response to back-arc extension (Cope et al., 1992; Leeder, 1988, 1982; Soper et al., 1987). Coastal erosion has exposed a series of abandoned underground workings on the headland (national grid square NX34 76) just north of St Mary's Lighthouse, Whitley Bay (England) (Fig. 2b). Whitley Bay is located in the Northumberland Trough, a 50 km wide, ENE-WSW trending, half graben which formed in response to the extensional reactivation of the Iapetus Suture during the mid to late Carboniferous (Chadwick et al., 1995; Chadwick and Holliday, 1991; Johnson, 1984). The thickest coal seams (>2 m), many of which are workable; (Fielding, 1982; Smails, 1935), are almost exclusively confined to the Pennine Middle Coal Measures which reach 450 m thick in places (C.R. Fielding, 1984; Leeder, 1974; Smails, 1935) (Fig. 2c).

Carboniferous lithologies at Whitley Bay consist of fossiliferous and barren mudstones (50 to 55%), siltstones and sandstones (40 to 48%) and bituminous coals (<5%), which nearly always occur above seat-earths (Christopher R. Fielding, 1984; Fielding, 1985, 1982; Jackson et al., 1985; Lawrence and Jackson, 1986). These are interpreted as being deposited on a broad, flat deltaic plain with numerous distributary channels (Christopher R. Fielding, 1984; Fielding, 1985; Jackson et al., 1985). Exceptional exposures of the Pennine Middle Coal Measures, including the

High Main Seam (HMS), are observed along the 1.2 km long studied section (British National Grid NZ 364 756; Figure 2b).

The High Main Seam is highly variable in thickness (average 2 m, Fielding, 1982) and quality (Christopher R. Fielding, 1984; Jackson et al., 1985; Lawrence and Jackson, 1986; Murchison and Pearson, 2000) with centimetre to meter scale shale partings commonly present (Fielding, 1982). Immediately below the HMS thin 'stringers' of coal (centimetre scale) are often found, which are locally workable (Fielding, 1982). Based on the history of the coalfield (Table 1), and because the workings are above the water table, we suggest the coal at Whitley Bay was extracted somewhere between 1550 and 1710 AD.

Date	UK wide	Northumberland and Durham Coalfields
Pre-1200	Extracted by shallow pits or adits (shallowly dipping tunnels)[1,2].	Workings of the high Main Seam date from Roman times[8].
1200s	Widespread coal mining began increasing up to, including and following the Industrial revolution.	Early shallow workings (<7 to 10 m) primarily using adits from the coast/valley side, with bell pits also used[9]
1300s	Bell-pits (Fig. 1a) became widespread[2,3].	
1500s	Most shallow reserves accessible by surface access methods extracted and the Pillar and Stall method began[2,3] (Fig. 1d).	1550's saw the increased extraction of the HMS, with coal becoming a significant commercial interest[3,10,11,12]. Pillar and stall workings began in the late 16th Century[2].
1600s		The majority of coal close to sea-ports and above the water table extracted by the late 17th Century[13].
1700s		Technological advances in 1710 enabled coal to be mined below the water table[13].
1800's	Mining methods became standardised[1,2] (Fig. 1b, c & e). In 1850 detailed coal mine surveys began, with abandonment plans becoming mandatory from 1872[1,4].	1800 map of sea-sale collieries does not include Whitley Bay workings[3]. 1830's to 1870s saw many large collieries opened up working the High Main Seam (e.g. Fenwick).
1900's		1993: Easington colliery closes marking the end of underground coal extraction in the Durham and Northumberland Coalfields.

Table 1: Summary of the mining history of the UK and Durham and Northumberland Coalfields. References; 1) Bell (1986), 2) Bruyn & Bell (1999), 3) Smails (1935), 4) Healy & Head (1984), 8) Fielding (1982), 9) Dearman et al. (2000), 10) Page (1907), 11) Smailes (1938), 12) Nef (1965), 13) Galloway (1898).

3 Methods

High-resolution sedimentary logs of 9 vertical sections, spaced every meter, were taken along the workings (see Figure 3). Lithological boundaries, both structural and depositional, were defined as either based on a distinct change in grain-size, or matrix type. A sedimentary log through the unworked High Main Seam at the base of Hartley Steps (British National Grid: NZ 34469 75668) was taken as the comparative baseline for the collapse lithologies. Facies were defined based on distinct changes in texture, grain size, stacking relationships and sedimentary structures. Collapse breccias were described using the terminology of Woodcock & Mort (2008), whereby chaotic-, mosaic- and crackle- breccias are defined based on clast size and ratio of clast to matrix. The clast type, orientation (taken as the dip of preserved bedding) and aspect ratio were recorded, along with the matrix composition. Muds in the sequence, which were not lithified, were described using the BS5930 (2015) standard for clay-rich soils.

In addition, photographs (320 images) were taken of the outcrop to create a high resolution, orthorectified, photomontage (Fig. 3). Using the sedimentological information and location of logged sections, key boundaries were mapped out and stacking relationships investigated. Within the collapse breccia, a number of sub-divisions could be defined with subtle changes in clast orientation observed (e.g. 45 and 82 cm in Log 1). These areas were used to help constrain the phases of collapse recorded in the sequence.

4 Results

4.1 General description

Through detailed field observations and sedimentary logging 8 facies were identified (Table 2). In this section, 'thickness' refers to the vertical thickness of a bed, pod, or lithology within the studied section. The relationship between sedimentary facies within the workings can be split into two areas, pillars and stalls, depending on whether unworked coal is present in the logged section (Fig. 3). Two stalls are present, which make up 69% of the outcrop, with similar facies associations observed above the High Main Seam in the central pillar, and edge of the northern pillar (Fig. 3).

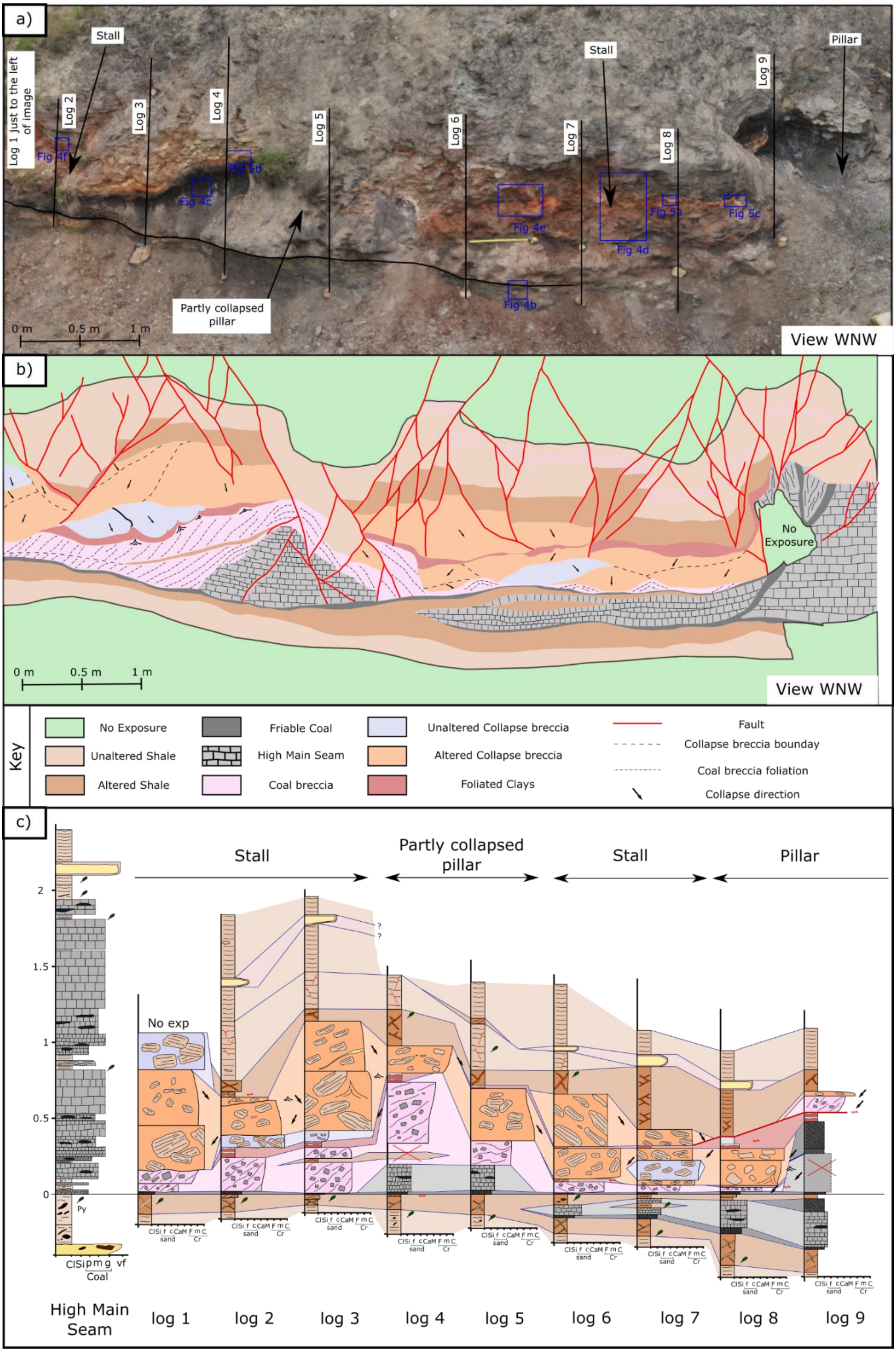

Figure 3: Workings of the High Main Seam at Whitley Bay: a) photomontage of the workings with the location of logs marked; b) section view and interpretation of mine wastes (collapse lithologies); and c) sedimentary logs through the undeformed High Main Seam at the base of Hartley Steps and through the workings at the locations marked in (a). For individual log descriptions please see Supplementary 1.

Facies	*Description*	*Depositional processes*
High Main Seam (HMS) Undeformed thickness = 2.01 m. Fig 4a	Interbedded unit containing 16 coal beds (2 to 43 cm thick) and 7 organic rich shale partings (1 to 4 cm thick). Euhedral pyrite crystals (<0.2 mm) occasionally visible along bedding planes. Locally Jarosite is developed along the cleat network, particularly towards the base of the High Main Seam.	The deposition of peat in a swampy, anoxic environment which was sporadically interrupted by clastic deposition in a delta plain environment[1].
Unaltered Shale (US) Beds 0.2 to 1 cm thick Fig 4b	A mudstone to silty-mudstone, which can be either organic rich or organic poor. Coalified plant fossils and euhedral pyrite (<0.2 mm, <5%) are often found along bedding surfaces, particularly below the HMS.	Low energy deposition in a variably oxic environment, related to the flooding of peat swamps[1,2].
Altered Shale (AS) Beds 0.2 to 0.8 cm Figs 4a & b	Found within 20 cm of the HMS in both undeformed and worked sections. Similar to US, however, weathers more readily and contains shallowly dipping alteration planes (yellow below & brick orange above).	The development of acid mine water following mining operation causes the degradation of clay minerals and movement of the sulfur from the pyrite within the seam[3].
Friable Coal (FC) <15 cm thick. Figure 4b & d	FC may be observed along the base, and within the workings, as well as along the edge of the right-hand pillar (Figure 3). FC is black, dominated by organic material (> 95%) and characterised by a very tight fracture network which cause the lithology to erode as a black powder. Fractures either occur perpendicular to layering, or at an angle forming a well-developed foliation.	Can either be formed by working related deformation of thin channel coals and stringers of the HMS or the development of tectonically deformed coals[4] along the edge of pillars during the collapse of workings.
Coal Breccia (CB) Thickness 2 to 55 cm Figure 4c	CB occurs along the base of the workings, and varies in thickness considerably. CB is a chaotic to mosaic breccia[5] consisting of angular clasts of coal (>90%) and highly altered shale. Coal clasts (median 60 mm^2) are bounded by bedding planes or cleats. Shale clasts are often altered to a red-orange, silt to clay grade dust. The matrix is dominated (<95%) by silt grade organic fragments with the remaining 5% consisting of quartz and occasional <0.5 mm pyrite crystals.	May be formed either a) through the spalling of the pillars, whereby talus-like deposits occur as pillars corrode through time[6] or b) through the down-dip flow of coal during flooding events being deposited in the lee side of pillar in a similar manner to bridge abutments[7].
Collapse Breccia (CoB) Thickness 20 to 90 cm Figure 4d & e	The dominant lithology in the collapsed stalls CoB is found as altered or unaltered pods of clast dominated (85 to 90%) crackle breccia[5]. Clasts, are dominated by shale clasts (90 %), with clasts of ironstone, coal and bleach-white sandstone or seat earth also present. Clasts typically show high aspect ratios elongated parallel to bedding. The matrix is clay-rich containing brick-orange, silt grade clasts of altered shale and sand grains.	Rotation of clasts away from pillars as material collapses into the stalls[8]. Where the permeably of the workings is low, and mine water develops, clays in the collapse breccia degrade and develop the orange alteration colour.

Foliated Muds (FM) *Thickness 0.5 to 15 cm* *Figure 4f & 5*	FM consists of mm to cm scale foliated muds which alternate between brick-red and off-white in coloration. Foliations typically stack from brick-red to white, with the top of the white foliations marking distinct depositional phases. Between 7 and 13 cycles can be identified, filling from the deepest point and occasionally showing soft-sediment deformation.	Cyclical flooding and evaporation of salt-rich fluids and mine water, causing a stacked sequence above the pre-existing CoB. The red foliations are likely caused by acid mine water reactions (see discussion for further details) forming Ochre deposits. Slumps develop either due to rapid deposition on the CoB top topography, or due to the further collapse along the workings.

Table 2: Facies description and interpretation of depositional environment. References: 1) Fielding (1984b); 2) Fielding (1982); 3) Younger et al. (2002); 4) Godyń (2016); 5) c.f. Woodcock & Mort (2008); 6) Martin & Maybee (2000); 7) Koken & Constantinescu (2008); 8) Lokhande et al. (2005).

4.2 Stalls

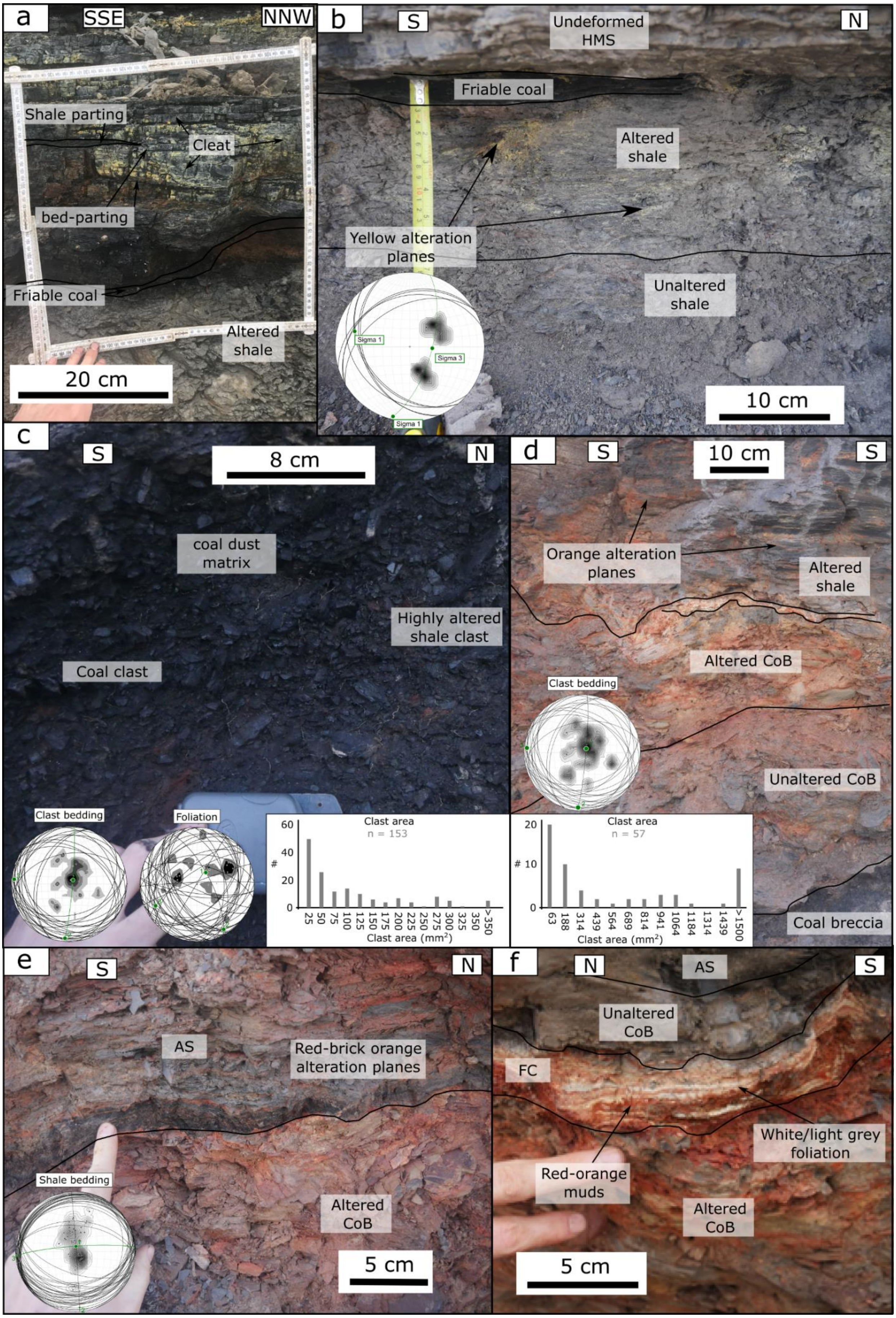
a
SSE
NNW
Shale parting
Cleat
bed-parting
Friable coal
Altered shale
20 cm
b
S
N
Undeformed HMS
Friable coal
Altered shale
Yellow alteration planes
Unaltered shale
Sigma 1
Sigma 3
10 cm
c
S
N
8 cm
coal dust matrix
Highly altered shale clast
Coal clast
Clast bedding
Foliation
Clast area
n = 153
Clast area (mm^2)
d
S
S
10 cm
Orange alteration planes
Altered shale
Altered CoB
Clast bedding
Unaltered CoB
Clast area
n = 57
Clast area (mm^2)
Coal breccia
e
S
N
AS
Red-brick orange alteration planes
Shale bedding
Altered CoB
5 cm
f
N
AS
S
Unaltered CoB
FC
White/light grey foliation
Red-orange muds
Altered CoB
5 cm

Figure 4: Facies photographs and associated clast and kinematic data. The location of the photographs for (b) to (f) is indicated on Figure 3. The photograph for (a) is taken at the base of Hartley Steps [British National Grid: NZ 34469 75668]. (a) undeformed High Main Seam with Jarosite developed along the cleats of the lowermost beds. (b) The succession underlying the High Main Seam, with the orientation of the yellow alteration planes shown in the inset stereographic projection. (c) Close up photograph of the coal breccia built up on the southern side of the central pillar. Inset stereographic projection display the orientation of clast bedding and the foliation picked out by fines. The inset histogram displays the equivalent circular area of all clasts measured in the field (n = 152). (d) The succession overlying the coal breccia. CoB = collapse breccia. The inset stereographic projection displays the orientation of bedding in the CoB clasts, with in inset histogram displaying the equivalent circular area of the clasts. (e) The contact between altered shale (AS) and Altered collapse breccia (CoB) at the top of the collapse lithologies. The insert stereographic projection displays the bedding of the altered and unaltered shale overlying the collapsed workings. (f) The development of the foliated muds above altered collapse breccia (CoB) towards the south of the outcrop.

The thickness of the collapsed stalls, defined as the distance between the laterally continuous friable coal, and the fractured unaltered shale at the top of the workings, ranges from 52 cm in log 7 to 114 cm in log 3 with the facies thicknesses and associations varying along the outcrop (Fig. 4c). The relationships of unaltered shale, altered shale and friable coal are the same as the undeformed section; however, the thickness of altered shale is greater beneath stalls. Coal breccia can be observed on-lapping onto the partially collapsed pillar (Fig. 4b), with the maximum thickness (c 40 cm) and larger clast sizes (median = 144 mm^2) found closest to the boundary of the pillar. Coal breccia does not show clear grading; however, a weak foliation is picked out by fines that dip down-dip and away from the pillar (Fig. 4c). Towards the south of the outcrop coal breccia occurs as a discontinuous layer, with the foliation suggesting that soft-sediment deformation caused by later collapses caused the thinning and thickening of the unit.

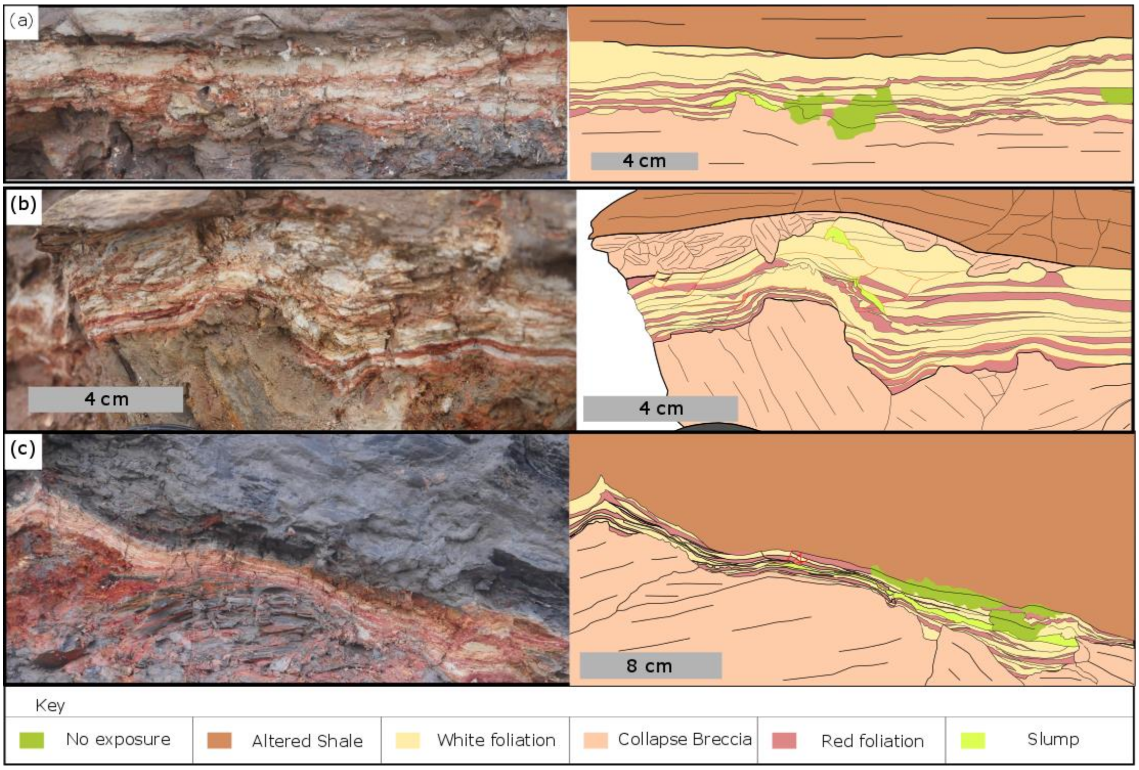

Figure 5: FC stacking patterns. The location of the detailed photographs are indicated on Figure 3. Please see text for a description of key features.

Foliated muds typically dip towards the SW and are observed in both stalls, overlying coal breccia in the south and either coal breccia or collapse breccia in the north. Complex stacking patterns and sedimentary structures are observed in the foliated muds, controlled by the underlying topography (Fig. 5). The alternating red- and white- layers are cyclical in nature, with the number of cycles varying from 7 to 13. At the base of foliated muds, the foliation can be seen on-lapping onto angular clasts of collapse breccia, with the thickest deposits occurring in gaps between clasts of collapse breccia (Fig. 3). This shows that the collapse occurred after mining and was followed by the deposition of the foliated muds, filling pods on the pre-existing topography on the top of collapse breccia. Stacking patterns in Fig. 5a suggest that rotation of this topography occurred throughout the deposition of the muds, leading to changes in depocenters probably caused by further collapse of workings disrupting the collapse breccia.

The bottom of the foliated muds is generally undisturbed, however, in the mid- to upper- sections of the deposit slumps, minor faulting and soft sediment deformation can be observed. Slumps occur where a paleoslope occurs either within the foliated muds or from the top of the collapse breccia. For example, in Fig. 5c a laterally extensive slump deposit is observed, with normal faults developed at its head, and compressional features at its foot. This can be observed along the shallowly dipping (c. 8° to 10°) upper surface of the collapse breccia. In Fig. 5b, the top of foliated muds has been deformed by a later collapse, which causes the soft-sediment deformation of a thick white layer, and small-scale faults and foliation rotation to occur.

Foliated muds may either be overlain by further collapses (collapse breccia), which often cause soft-sediment deformation of the pre-existing units, or to the far north by altered shale. Altered shale makes up the top of the collapse lithologies and is brought down onto underlying lithologies by a series of fault strands that lead to the closing of open space (Fig. 5b) and the extrusion of foliated muds along the edge of the pillar (Fig. 6a).

4.3 Pillars

Two pillars, which make up 31% of the outcrop, are observed, one to the north and another near the centre of the studied section. In the northern outcrop, the top 0.45 m of the undeformed High Main Seam succession is observed and the base is visible in the foreshore up-dip of the studied section; suggesting that the full thickness of the seam (c. 2 m) is present at this location. The base of the High Main Seam exposed in the centre of the outcrop (logs 4 and 5) closely matches the log of the undeformed sequence (Fig. 3c). However, above the undeformed coal in log 4 and 5, 14 to >40 cms of coal breccia are observed. This displays a subtle foliation, which dips away from the pillar and contains semi-randomly orientated clasts (Fig. 4c). Above the coal breccia, the central pillar shows facies associations more similar to that observed in the stalls (see above). The unaltered shale at both locations display low-amplitude folding (Fig. 4e), with material subsiding from above the pillars into stalls (See Fig. 3).

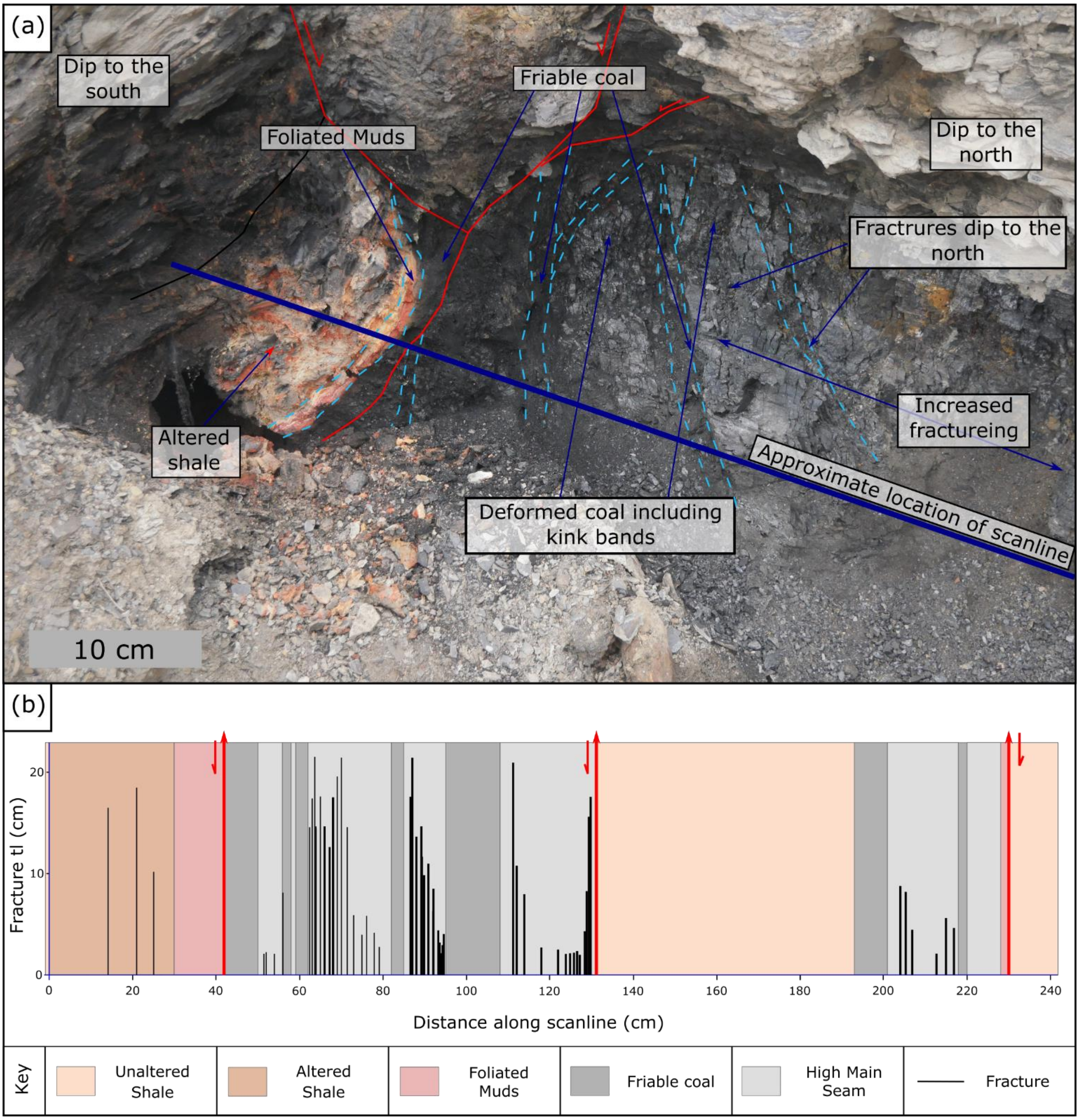

Figure 6: Northern Pillar: a) annotated field photograph displaying key structural elements of the edge of the northern pillar; b) scanline through the edge of the pillar displaying the trace length of fractures. The location of the scanline is highlighted in a.

The High Main Seam in both pillars displays increased fracturing compared to the undeformed section, along with local development of friable coal (Fig. 6). The scanline taken through the northern outcrop (Fig. 6b), highlights that within 5 cm of the friable coal the trace length and intensity of fractures increases. Fractures are often observed to form parallel to, and utilising the pre-existing cleat network. Locally, particularly between strands of friable coal, the rotation of coal, including cleats, fractures, and coal bedding is observed (Fig. 6a). This suggests that fracturing occurred prior to the block rotation of the coal, and that only later deformation (e.g. development of kink-bands) occurred during the development of friable coal.

Bedding orientation below the High Main Seam is similar to the seam itself (040°/10° W), however, bedding above the seam maintains thickness and dips to the north and south with a mean fold axis of 105°/80° N (Insert Fig. 4a). Folding is subtle above stalls, however, above pillars it is clearly visible. At this location the folding and rotation of bedding along antithetic faults occurs such that two anticlines and three synclines with wavelengths of 0.5 m to 2 m are observed. We suggest folding is due to the rotation of the overburden following roof collapse.

5 Discussion

5.1. Processes involved in the formation of collapsed pillar and stall workings

We investigated the processes which occur during the collapse of abandoned pillar and stall mine workings. This has allowed for the first time the development of a conceptual evolutionary model for the temporal evolution of the internal structure be proposed. We find that the collapse at Whitley Bay occurred through five distinct phases, as evidenced by sedimentary facies and associations, deformation style and sedimentary structures. The stages are outlined below and summarised in Fig. 7.

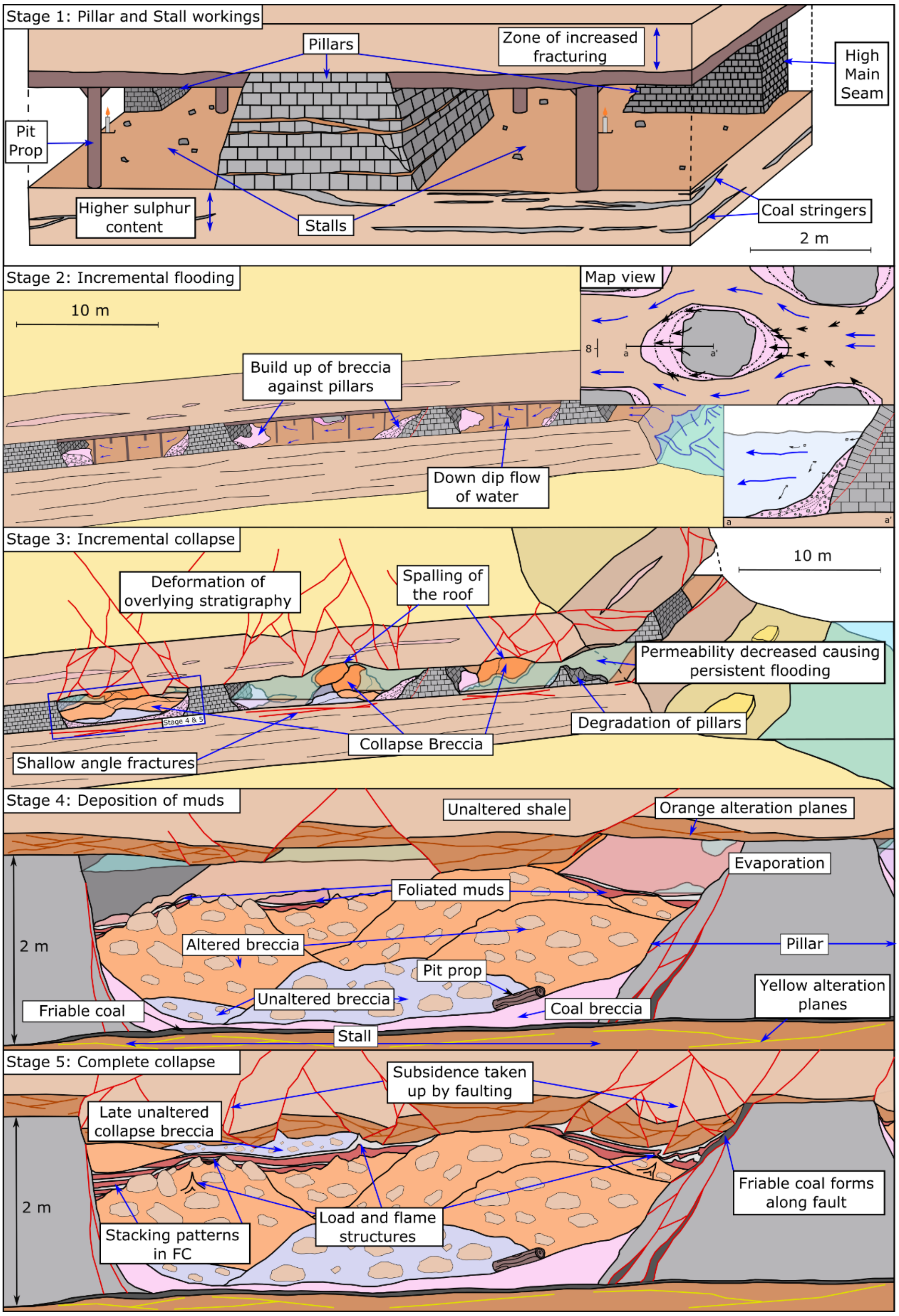

Figure 7: Conceptual evolutionary model of the collapse of pillar and stall mine workings based on Whitley Bay, Northumberland. See text for description of each stage.

<u>Stage 1 & 2: Extraction of coal and build-up of CB:</u>

Estimated between 1550 and 1710 AD (see Table 1), the High Main Seam was worked using pillar and stall mining methods. The shallow depth of the seam at this location suggests that access was most likely from an adit cut from the sea. Coastal erosion rates in the area range between 0.15 to 0.30 cm per year

(Tingay and Ellis, 2016), suggesting that a minimum of between 46.5 m and 93 m of rock has been eroded since the mine was developed. Assuming no disruption due to faulting in the eroded section and disregarding isostatic uplift and recent seal level rise, the seam would have been 8 to 10 m above the mean high-water mark. Lying above the water table, workings would not need to be pumped but designed to drain under gravity via adits, so flooding would only have occurred following periods of heavy rain or winter storms. During the extraction of coal, small fragments of low-value coal and coal dust would be left behind. These would have been transported down-stream (towards the SW) during flood events and deposited against pillars, leading to the development of the coal breccia. The on-lapping of coal breccia onto the degraded pillar (Fig. 3b), orientation of the faint foliation (Fig. 4c), and clast-bedding orientation (Fig. 4c) matches the deposition pattern you would expect in a shallow channel flowing around an obstacle (e.g. scouring around vertical dikes (Koken and Constantinescu, 2008)). separation of coal be density to form a coal "lag" is typical in streams and beaches. Following the end of mining operations upkeep was no longer required, and pillars began to spall and collapse (Ebrahim F Salmi et al., 2019). Larger, high value, clasts of coal would then added to the breccia (**Stage 2**).

<u>Stage 3: Incremental collapse and steady reduction in permeability:</u>

As time passed, episodic flooding degraded pillars and pit-props and the roof of the workings began to sag and spall (e.g. Bruyn & Bell 1999). In agreement with the work of Helm *et al.* (2013), we find collapse initiated near the centre of stalls, which were only held up by pit-props, followed by several small collapses propagating towards the pillars. Initially collapses did little to reduce the overall permeability of the workings, and episodic flood waters would flow around the collapsed sections. As the percentage of collapsed material increased, clays sourced from shales would clog pore-space between clasts. The breccia, which was poorly sorted and already had a low permeability, would have become saturated.

Mine water is typically acidic and can represent a significant environmental risk if it leaks into surface and/or groundwater resources (Younger, 2004, 1995). The acidity of mine-waters is a product of both 'vestigial acidity' caused by the past oxidation of pyrite, and 'juvenile acidity' caused by the products of seasonal pyrite oxidation above a fluctuating water table (Younger, 1998). A complex cycle of chemical reactions takes place as pyrite oxidises (See Stumm and Morgan, (1981) for full description). However, the simplified net products can be described through Equation 1, with the overall sequence being acid-producing (Equation 2) (Banks et al., 1997):

$$2FeS_2 + 2H_2O + 7O_2 = 2Fe^{2+} + 4SO_4{}^{2-} + 4H^+{}_{(aq)} \quad \text{(Equation 1)}$$

$$Pyrite + water + oxygen = ferrous\ iron + sulphate + acid$$

$$4FeS_2 + 14H_2O + 15O_2 = 4Fe(OH)_3 + 8SO_4{}^{2-} + 16H^+{}_{(aq)} \quad \text{(Equation 2)}$$

While little pyrite oxidation will take place below the water level, oxidation will be abundant in the unsaturated zone with the reaction products mobilised as ground water rises (Younger, 1993; Younger and Sherwood, 1993). The high acidity and oxidising environment represents the ideal situation for the development of Ochre (Younger et al., 2002). Ferrous iron released by the oxidation of pyrite will remain in solution while acidity is particularly high (pH < 2.5) or where oxygen levels are reduced (e.g. fully saturated workings) (Banks et al., 1997; Younger et al., 2002). However, when the ferrous iron is exposed to the atmosphere partial oxidation will occur leading to the precipitation of ion oxyhydroxide (Ochre) (equation 3 and 4) (Banks et al., 1997).

$$4Fe^{2+} + O_2 + 4H^+ \rightarrow 4Fe^{3+} + H_2O \quad \text{(Equation 3)}$$

$$Fe^{3+} + 3H_2O = FeOOH + H_2O + 3H^+ = Fe(OH)_3 + 3H^+ \quad \text{(Equation 4)}$$

The pyrite within the saturated collapse breccia, would have been oxidised to form weakly acidic mine waters (Turner and Richardson, 2004; Younger, 1995, 1994), that altered clays in the matrix and clasts of the collapse breccia and mobilised iron from the ironstone nodules/beds. This oxidation and leaching caused the red-orange coloration and bleaching respectively. The presence of breccia pods that do not show alteration suggests that some earlier and later collapses did not become saturated, potentially due to being above the water level or lacking hydrogeological connections with mine water. Onlapping relationships suggest the collapse at Whitley Bay occurred through a total of 19 events (Fig. 3b).

Stage 4: Formation of the foliated muds.

The fluid which formed the foliated muds was apparently hyper-saline and displayed cyclical variability in composition. As there was no flow, clays settled from suspension, and became deposited as a thin layer of mud (the red foliation) (Figures 4 and 5). The orange-red colour and silt-grade grains are similar to the altered shale clasts in the coal breccia, and likely represent clays sourced from shales altered by acid mine waters (c.f. Younger 1995). The top of each cycle is white to off white, clay-rich layers with a distinctly salty taste and appeared to contain precipitates. The deposits first built up as small pods in topographic lows on top of collapse breccias, suggesting that the hyper-saline fluid formed puddles on the breccia, and deposition through evaporation occurred prior to the next pulse. This type of deposit is commonly seen where brines periodically flood areas of topography (in this case the mine floor), essentially acting as a mini-basin which is infilled during reflux (Warren, 2016).

In the Durham and Northumberland coalfields, the presence of hypersaline barite rich brines have been reported (Younger, 1995). Locally this has led to the development of Baryte ($BaSO_4$) and Witherite ($BaCO_3$) veins within the Westphalian Coal Measures (Dunham, 1983), which are locally mined (Dunham, 1948). The Eccles Colliery, located 5.5 km west of the field site (British National Grid = NZ 304 695), primarily worked both the Main and High Main Seams and had problems with barium-rich groundwater (Grey and Judd, 2003). This required the installation of a Blanc-fixé plant that produced around 3000 tons of $BaSO_4$ per year (Palumbo-Roe and Colman, 2010). Alternation of Ba-rich brines with acidic minewaters could have led to the alternate deposition of baryte and ochre in the abandoned mineworkings, mimicking the mixing reaction used for the industrial process. Witherite is almost exclusively produced through the precipitation of barium sulphide solutions with either carbon dioxide (equations 5 & 6) or soda (Kresse et al., 2007). CO_2, locally termed blackdamp, is abundant within coalmine workings and the evidence at Whitley Bay suggests the workings were periodically flooded, providing H_2O into the system (Stage 1-3). Therefore, the conditions were present for the precipitation of witherite from upwelling barium rich hypersaline fluids , given the likely presence in the mineworkings of sulphate-reducing bacteria.

$$2BaS + CO_2 + H_2O = BaCO_3 + Ba(HS)_2 \qquad \text{(Equation 5)}$$

$$Ba(HS)_2 + CO_2 + H_2O = BaCO_3 + 2H_2S \qquad \text{(Equation 6)}$$

Due to the presence of both altered and unaltered collapse breccia, we suggest that the water table, and hence the composition of groundwater, varied annually. As groundwater levels rise due to meteoric water inputs, the products of pyrite oxidation will dissolve and the acidity of the groundwater will increase (as discussed in Stage 3). This will cause the proportion of acidic mine water relative to brines to increase and promote the breakdown of clays within the shales (Younger et al., 2002), which become entrained into the hypersaline fluid and carried in suspension. When the meteoric input and flow rate decreased, dropping water levels lead to the deposition of the red-mud layer. At times when pyrite oxidation was lower, the brine component of groundwater dominated and less clays were held in suspension. This led to the deposition/precipitation of salty muds (possibly with light-coloured baryte or witherite precipitates) in place of the red muds. Due to the likely annual variation in the occurrence of highly saline brines, and the periodicity observed in the foliated muds we suggest foliated muds were annular deposits over a 7 to 13 year period.

Slump-deposits and soft sediment deformation within foliated muds occurs either a) where the dip of the paleo-topography is high (>8°), or b) in the vicinity of later collapse breccia pods (Fig. 5). Slump deposits may either be caused by the rapid build-up of sediment on a slope (Moore, 1961), or following ground motions, for example earthquakes (Keefer, 1984). Both processes could have been active in the workings, with pulses of saline brines and/or flooding during winter storms causing rapid deposition of muds and evaporites and ground motion caused by roof collapse. The slump deposits in both Fig. 5a and b show no disruption of overlying layers, and have upright folds at the toe following an 'open-toe' deposition style with units above on-lapping onto the deposit (c.f. Alsop *et al.* 2016). In contrast the deposit in Fig. 5c has a longer run out, is thicker and overlying cycles are deformed through normal faulting at the head and compressional features at the toe. We suggest the slumps in Fig. 5 a and b formed due to rapid sedimentation on the paleo-topography present on the top of the collapse breccia, possibly triggered by minor collapses. Fig. 5c, however, was deposited following a roof collapse which caused a slump to develop, utilising a shallowly dipping clay layer as a decollement, similar to large scale processes caused by earthquakes (Alsop et al., 2016). Collapse related slumps are found at different stratigraphic layers within the foliated muds, suggesting the workings collapsed over several years.

Stage 5: Final collapse of stall:

Eventually pillars degraded to the point where they could no longer support the overlying stratigraphy and the roof collapsed. The collapse and subsidence of overlying units is accommodated through normal faults which dip away from the zone of collapse. This caused triangular zones of deformation, with subsidiary faults coming off the main strands (Fig. 3). The minor faulting pattern was controlled by the topography of the pre-existing collapse lithologies. For example, to the north of the partially collapsed pillar material was brought down by several small-offset fault strands which bound 'lenses' (c.f. Gabrielsen *et al.* (2016)) of undeformed shale and ironstone.

The orange alteration of the collapse lithologies at Whitley Bay (Fig. 4) suggests that they were at least partially saturated at the time of collapse, with soft sediment deformation observed in collapse breccias, foliated muds, and coal breccias (Figs. 3b, 5). While Stage 5 occurred following the deposition of foliated muds to the north of the outcrop, in the rest of the outcrop Stage 4 is followed by a return of Stage 3 and the deposition of collapse breccia pods (Fig. 3). Where collapse breccia is not found, foliated mud is thickest with the greatest number of cycles observed (13 as compared to 7 to 8 to the south). This suggests that the void near pillars was open to flow far longer that the rest of the workings. If our interpretation that the cycles represent annual pulses of saline-rich brines is correct this then suggests the stall closest to the pillar remained a conduit for flow six years longer than the centre of the void.

While the exact stacking patterns at Whitley Bay are representative of a single location, the processes are likely comparable to other pillar and stall workings. Abandoned coal mines in the UK are known to have collapsed following post-mining groundwater recharge (e.g. Bathgate, (Carter et al., 1981)) and the degradation of the pit props (Donnelly, 2006) with collapses remaining a major geotechnical risk to this day (Donnelly et al., 2009; Gee et al., 2017; Helm et al., 2013). Stage 4 (the deposition of foliated muds) may not be widely observed and occurs at Whitley Bay because the workings were above a variable water table influenced by cyclical pulses of deep saline brines. Previous work has suggested that collapse occurs as a single event, over days to weeks (Carter et al., 1981; Marino and Gamble, 1986), however, our data suggests that at-least part of the workings remain open to flow for a significantly longer period of time (7 to 13 years). Wide spread regional subsidence in ex-mining areas is well known (e.g. Gee *et al.* (2017)), but it may be that these small sections which remain open to flow are not large enough to cause noticeable surface deformation when they fail.

5.2 Comparison between the sedimentology of mine and cave collapse.

A good analogue for the lithologies and processes described in this study is the collapse and sedimentation of modern and paleo-cave systems (e.g. (Labourdette et al., 2007; Loucks, 2007, 1999; Mcmechan et al., 2002). Loucks *et al.* (2004) identified 5 paleo-cave facies from core and outcrop data which display distinct properties showing clear parallels to the facies observed at Whitley Bay (Table 3). The key differences in the depositional systems include: the thickness and lateral extent of the facies; properties of the zone of damage; initial lithological properties; and finally that the collapsed mine workings leave a low permeability, clay-rich layer and not a highly permeable coarse chaotic collapse breccia (Loucks et al., 2004).

Cave collapse facies Louchs et al. (2004)	**Equivalent mine collapse facies identified in this study**
Continuous Strata Facies: Competent, coherent bedded carbonates, with only local evidence of deformation.	Interbedded siliciclastic lithologies with high clay content in the succession.
Discontinuous Strata Facies: Characterised by localised folding and faulting, with some local brecciation. Bedding is generally continuous along strikes. The unit is highly fractured and has local development of mosaic breccia.	Localised faulting and the rotation of bedding is observed; however, bedding can still be observed.
Highly Disturbed Strata Facies: Highly deformed, discontinuous bedded strata with considerable amounts of crackle and mosaic brecciation. Small scale fault and folding common and interbeds of clastic material mark where individual collapse events are recorded.	Immediately above the worked seams deformation quickly interacts with deformation patterns from nearby stalls (Stage 3), which will only occur in caves where two sections of caves are in close proximity.
Coarse-Clast chaotic breccia facies: Very poorly sorted, matric to clast-supported granule-to boulder-sized chaotic breccia. Finer interbeds common, interpreted as sediment transport into the cave (Loucks, 1999). Overall volume of collapsed lithology increase by c. 40% (Labourdette et al., 2007). Where available rock is less than 2.5 times the volume a collapse sinkhole develops (e.g. Mylroie et al., 1991; Harris et al., 1995).	Similar to the collapse breccia, however, due to the shale roof of the High Main Seam, lower expansion of the breccia occurs during collapse, permeability will be low and only a small space is available to be filled with fines. The collapse of shallow workings can lead to sink hole development (Garrard and Taylor, 1988; Poulsen and Shen, 2013).
Fine Chaotic Breccia: Poorly to well sorted, matrix to clast-supported, granule- to cobble-sized chaotic breccia. Sediment fill commonly observed, but limited to small grain size. Sediment fill deposited by transport from within or outside the cave (Loucks, 1999).	Coal breccia develops from material left from mining operations and the spalling of pillars (Martin and Maybee, 2000). This then gets transported along the coal seam.
Finer Grained Sediment Facies: Consist of silt- to granular-size sediment, dominated by detrital carbonate. Siliciclastic clay may reach 4%, but generally accounts for less than 1%. Sediment is interpreted as being transported in an open chamber by traction, mass-flow and suspension mechanisms.	Foliated muds get deposited from the mixing of mine-waters and deep hyper-saline brines leading to the sedimentation of thin muds from evaporation, suspension and mass transport mechanisms.

Table 3: Comparison between cave collapse lithologies and those observed in this study.

5.3. Implications for shallow mine geothermal

Ground water flow through abandoned mine workings can be considerable; for example, discharge flow rates from the workings of the Shilbottle Seam in Northumberland (UK) ranged from 0.8 ML/d to 2.6 ML/d (median = 1.7 ML/d) (Younger, 2004). Our work shows that where flow can occur along stalls prior to flooding, any collapse, including early spalling of the roof, adds low permeability, clay-rich, lithologies to the system. Within the collapsed breccia, several distinct packages were observed, occasionally showing alteration. This shows that Stage 3 did not occur instantaneously, instead representing a gradual decrease in void space, the migration of the void upwards, and the development of a topography at the base of the seam associated with the sagging and spalling of the roof. During this time flow would still occur, however, whilst workings are only partly flooded, fluid pathways would become longer and localised around pillars.

The presence of cycles within the foliated muds suggest that undersaturated fluid flow occurred over a period of 7 to 13 years. However, this might be a low estimate as it is not clear when pulses of hypersaline brines began. For deeper workings this could also be triggered by regional groundwater rebound following the end of mining operations (Burke and Younger, 2000). The thickest deposits of FM are in the vicinity to pillars, suggesting that this is the best location for flow, particularly as collapse in these areas occurs later than the rest of the workings. It is important, however, to consider not only the permeability of the lithologies which make up the mine workings, but also fracture networks which can combine to form flow pathways (e.g. McCay *et al.* 2019). Pillars display increased fracturing compared to the undeformed section (Fig. 6), and the low angle faults which bring the final collapse propagate from the pillars into overlying units (Fig. 3). Tectonically deformed coal, which may occur along the edge of pillars (Figs. 3 & 6), has a significantly reduced permeability (Ju and Li, 2009) which will inhibit flow into stalls. While large open voids remain, the water capacity and permeability of the flooded workings will remain high; however, after the final stages of collapse (post stage 3/4) the mine will become increasingly less viable as a geothermal reservoir.

After mine abandonment the level of the seam is generally well constrained (Table 1), however, the location, arrangement, and composition of pillar and stalls is often unknown (Bruyn and Bell, 1999). Likewise, the current level of minewater might not reflect the flooding history. This uncertainty is of particular importance for commercial geothermal projects due to the high cost of drilling (Lukawski et al., 2016), with the geothermal potential of a well differing considerably depending on if you intersect a pillar, open stall, or collapsed stall. Where a stall is encountered, the fill type will depend on the stage of collapse and vary considerably along strike (Fig. 3). In general, the presence of a clay-rich collapse breccia will be a sign of at least partial collapse and the presence of shale and sandstone fragments/core with a brick-orange coloration suggests that perched mine waters have developed prior to full saturation of the collapse lithologies and began to form low-permeable clay layers. Although the collapse lithologies and clay layers have low permeability, they are also highly plastic and poorly consolidated. During mine dewatering or minewater rebound it is common to observe rapid break outs of collapsed roof-fall debris. For example, Younger (2002) reported that the large uncontrolled release of acidic mine water from the Wheal Jane abandoned tin mine was caused by dewatering removing collapsed roof material that hydraulically connected two sections of the mine. This suggests that blockages caused by the collapse of stalls could be cleared, and void spaces connected through surcharging or the pumping of high-pressure water to dislodge the plastic clays and collapse breccias.

We show that the future water capacity and permeability of unsaturated pillar and stall workings decreased as the degradation of pillars cause the roof to sag, spall, and eventually collapse. Workings in the final stages of collapse (post stage 3; Fig. 7), have a greatly reduced volume for fluid flow, and an increased number of potential flow pathways into overlying units. When assessing a site for geothermal potential it is therefore integral that the phases of collapse and flooding are considered. These findings combined with those outlined by Malolepszy (2003) will be key for assessing the water capacity and permeability structure of target workings.

6 Conclusions

We present for the first time a detailed study of the internal structure of a collapsed pillar and stall coal mine. The internal structure of the workings at Whitley Bay comprises of 8 distinct facies, with lithology, kinematics, stacking patterns and structure informing the collapse processes. A 5-stage model of stall collapse is proposed, each acting to decrease the permeability of the mine. Stage 1 represents the methods used in initial coal extraction, and provides the initial framework for the rest of the collapse, during this time small fragments of coal were deposited on the seam floor, which increased in size when the seam was abandoned (Stage 2). Following working (Stage 3) the roof began to spall, gradually collapsing through multiple events (at least 19 at Whitley Bay), and acid mine water began to form. In Stage 4 the presence of hypersaline brines led to the cyclical deposition salty muds. Assuming annual cyclicity, this suggests that the stalls were open to unsaturated flow for at least 7 to 13 years. Finally (Stage 5), the roof collapses along several normal faults, which form triangle zones and lead to the subsidence of the overlying stratigraphy. The last section to collapse is closest to the pillar, occurring 6 years after the rest of the workings.

Our findings have significant implications for the shallow mine geothermal sector, raising a number of factors which need to be considered when assessing a potential site. Even when a stall is intersected the stage of collapse will affect whether significant flow can be maintained. The water capacity and permeability of a potential mine geothermal site degrades through time as the roof spalls, and finally collapses. The well-connected fault and fracture network which overlies the workings can enhance or degrade the geothermal potential of a site. While this work is limited to a single unsaturated site, we suggest the processes are widespread and apply to deeper workings prior to final abandonment and flooding. We propose that pillar and stall workings be considered as a heterogeneous, clay-rich anthropogenic layer whereby properties vary through time as collapse progresses.

References

Alsop, G.I., Marco, S., Weinberger, R., Levi, T., 2016. Sedimentary and structural controls on seismogenic slumping within mass transport deposits from the Dead Sea Basin. Sediment. Geol. 344, 71–90. https://doi.org/10.1016/j.sedgeo.2016.02.019

Banks, D., Athresh, A., Al-Habaibeh, A., Burnside, N., 2019. Water from abandoned mines as a heat source: practical experiences of open- and closed-loop strategies, United Kingdom. Sustain. Water Resour. Manag. 5, 29–50. https://doi.org/10.1007/s40899-017-0094-7

Banks, D., Younger, Paul L, Road, H., Younger, P L, Arnesen, R.-T., Iversen, E.R., Banks, S.B., 1997. Mine-water chemistry: the good, the bad and the ugly. Environ. Geol. 32, 157–174. https://doi.org/https://doi.org/10.1007/s002540050204

Bell, F.G., 1986. Location of abandoned workings in coal seams. Bull. Int. Assoc. Eng. Geol. 33, 123–132. https://doi.org/https://doi.org/10.1007/BF02594714

Bruyn, F.G., Bell, D.I.A., 1999. Subsidence problems due to abandoned pillar workings in coal seams. Bull. Eng. Geol. Environ. 57, 225–237.

BSi, 2015. BS 5930 - COP for ground investigations. BSi Standards Ltd.

Burke, S.P., Younger, P.L., 2000. Groundwater rebound in the South Yorkshire coalfield: a first approximation using the GRAM model. Q. J. Eng. Geol. Hydrogeol. 33, 149–160. https://doi.org/10.1144/qjegh.33.2.149

Carter, P., Jarman, D., Sneddon, M., 1981. Mining Subsidence in Bathgate, a Town Study, in: Gredds, J.D. (Ed.), Proceedings of the Second International Conference on Ground Movements and Structures. Pentech Press, London, Cardiff, pp. 101–124.

Chadwick, B.A., Holliday, D.W., Holloway, S., Hulbert, A.G., Lawrence, D.J.D., 1995. The structure and evolution of the Northumberland-Solway Basin and adjacent areas. London:HMSO.

Chadwick, R.A., Holliday, D.W., 1991. Deep crustal structure and carboniferous basin development within the iapetus convergence zone, northern England. J. Geol. Soc. London. 148, 41–53. https://doi.org/10.1144/gsjgs.148.1.0041

Cope, J.C.W., Ingham, J.K., Rawson, P.F., 1992. Atlas of palaeogeograpy and lithofacies. Geol. Soc. London Mem. No. 13.

Daunton, M.J., 1981. Down the pit: work in the Great Northern and South Wales coalfields, 1870-1914. Econ. Hist. Rev. 34, 578–597.

Dearman, W.R., Money, M.S., Strachan, A.., Coffey, J.R., Marsden, A., 2000. A regional engineering geological map of the Tyne and Wear County, NE England. Bull. Int. Assoc. Eng. Geol. 19, 5–17.

Dochartaigh, B.E.O., 2009. A scoping study into shallow thermogeological resources beneath Glasgow and the surrounding area. Br. Geol. Surv. Res. Rep. IR/09/024, 17pp.

Donnelly, L.J., 2006. A review of coal mining induced fault reactivation in Great Britain. Q. J. Eng. Geol. Hydrogeol. 39, 5–50.

Donnelly, L.J., Culshaw, M.G., Bell, F.G., 2008. Longwall mining-induced fault reactivation and delayed subsidence ground movement in British coalfields. Q. J. Eng. Geol. Hydrogeol. 41, 301–314. https://doi.org/10.1144/1470-9236/07-215

Donnelly, L.J., Culshaw, M.G., Bell, F.G., Tragheim, D., 2009. Ground deformation caused by fault reactivation: some examples, in: The 10th IAEG International Congress. Nottingham, UK, pp. 1–13.

Fielding, C.R., 1985. Coal depositional models and the distinction between alluvial and delta plain environments. Sediment. Geol. 42, 41–48.

Fielding, C.R., 1984. Upper delta plain lacustrine and fluviolacustrine facies from the Westphalian of the Durham coalfield, NE England. Sedimentology 31, 547–567.

Fielding, Christopher R., 1984. A coal depositional model for the Durham Coal Measures of NE England. J. Geol. Soc. London. 141, 919–931.

Fielding, C.R., 1982. Sedimentology and stratigraphy of the Durham coal measures, and comparisons with other British coalfields. Durham University.

Gabrielsen, R.H., Braathen, A., Kjemperud, M., Valdresbraten, M.L.R., 2016. The geometry and dimensions of fault-core lenses. Geol. Soc. London, Spec. Publ. 439, 1–21. https://doi.org/10.1144/SP439.4

Galloway, R.L., 1898. Annals of Coal Mining and the Coal Trade, Vol 1. ed. London.

Garrard, G.F.., Taylor, R.K., 1988. Collapse mechanisms of shallow coal-mine workings from field measurements. Geol. Soc. London, Eng. Geol. Sprecial Publ. 5, 181–192.

Gee, D., Bateson, L., Sowter, A., Grebby, S., Novellino, A., Cigna, F., Marsh, S., Banton, C., Wyatt, L., 2017. Ground Motion in Areas of Abandoned Mining : Application of the Intermittent SBAS (ISBAS) to the. Geosciences 7, 1–26. https://doi.org/10.3390/geosciences7030085

Godyń, K., 2016. Structurally Altered Hard Coal in the Areas of Tectonic Disturbances – An Initial Attempt at Classification. Arch. Min. Sci. 61, 677–694. https://doi.org/10.1515/amsc-2016-0047

Hamm, V., Sabet, B.B., 2010. Geothermics Modelling of fluid flow and heat transfer to assess the geothermal potential of a flooded coal mine in Lorraine , France. Geothermics 39, 177–186. https://doi.org/10.1016/j.geothermics.2010.03.004

Healy, P.R., Head, J.M., 1984. Construction over abandoned mine workings. No 34.

Helm, P.R., Davie, C.T., Glendinning, S., 2013. Numerical modelling of shallow abandoned mine working subsidence affecting transport infrastructure. Eng. Geol. 154, 6–19. https://doi.org/10.1016/j.enggeo.2012.12.003

Jackson, I., Lawence, D.J.., Frost, D.V., 1985. Geological notes and local details for Sheet NZ 27 Cramlington, Killingworth and Wide Open (SE Northumberland). Mem. Br. Geol. Surv. Sheets 14.

Johnson, G.A.L., 1984. Subsidence and sedimentation in the Northumberland Trough. Proc. Yorksh. Geol. Soc. 45, 71–83.

Ju, Y., Li, X., 2009. New research progress on the ultrastructure of tectonically deformed coals. Prog. Nat. Sci. 19, 1455–1466. https://doi.org/10.1016/j.pnsc.2009.03.013

Keefer, D.K., 1984. Landslides caused by earthquakes. GSA Bull. 95, 406–421. https://doi.org/10.1130/0016-7606(1984)95<406:lcbe>2.0.co;2

Koken, M., Constantinescu, G., 2008. An investigation of the flow and scour mechanisms around isolated spur dikes in a shallow open channel: 1. Conditions corresponding to the initiation of the erosion and deposition process. Water Resour. Res. 44. https://doi.org/10.1029/2007WR006489

Kresse, R., Baudis, U., Jäger, P., Riechers, H.H., Wagner, H., Winkler, J., Wolf, H.U., 2007. Barium and Barium Compounds, in: Ullmann's Encyclopedia of Industrial Chemistry. Wiley-VCH Verlag GmbH & Co. KGaA, Weinheim, Germany. https://doi.org/10.1002/14356007.a03_325.pub2

Labourdette, R., Lascu, I., Mylroie, J., Roth, M., 2007. Process-like modeling of flank-margin caves: from genesis to burial evolution. J. Sediment. Res. 77, 965–979. https://doi.org/10.2110/jsr.2007.086

Lawrence, D.J.., Jackson, I., 1986. Geology of the Ponteland-Morpeth District. Mem. Br. Geol. Surv. Sheets 9 a.

Leeder, M.R., 1988. Recent developments in Carboniferous geology: a critical review with implications for the British Isles and N.W. Europe. Proc. Geol. Assoc. 99, 79–100.

Leeder, M.R., 1982. Upper Palaeozoic basins of the British Isles-Caledonide inheritance versus Hercynian plate margin processes. J. Geol. Soc. London 139, 479–491. https://doi.org/10.1144/gsjgs.139.4.0479

Leeder, M.R., 1974. Lower border group (Tournaisian) fluvio-deltaic sedimentation and palaeogeography of the Northumberland basin, in: Proceedings of the Yorkshire Geological Society. pp. 129–180. https://doi.org/10.1144/pygs.40.2.129

Lokhande, R.D., Prakash, A., Singh, K.B., Singh, K.K.K., 2005. Subsidence control measures in coalmines : A review 64, 323–332.

Loredo, C., Ordóñez, A., Garcia-ordiales, E., Álvarez, R., Roqueñi, N., Cienfuegos, P., 2017. Science of the Total Environment Hydrochemical characterization of a mine water geothermal energy resource in NW Spain. Sci. Total Environ. 576, 59–69. https://doi.org/10.1016/j.scitotenv.2016.10.084

Loredo, C., Roqueñí, N., Ordóñez, A., 2016. Modelling flow and heat transfer in flooded mines for geothermal energy use: A review. Int. J. Coal Geol. 164, 115–122. https://doi.org/10.1016/j.coal.2016.04.013

Loucks, R.G., 2007. A Review of Coalesced , Collapsed-Paleocave Systems and Associated Suprastratal Deformation. Acta Carsologica 36, 121–132.

Loucks, R.G., 1999. Paleocave carbonate reservoirs: origins, burial-depth modifications, spatial complexity and reservoir implications. Am. Assoc. Pet. Geol. Bull. 83, 1795–1834.

Loucks, R.G., Mescher, P.K., Mcmechan, G.A., John, A., Jackson, K.G., Veritas, P.K.M., Drive, P., 2004. Three-dimensional architecture of a coalesced , collapsed- paleocave system in the Lower Ordovician Ellenburger Group , central Texas 5, 545–564. https://doi.org/10.1306/12220303072

Lukawski, M.Z., Silverman, R.L., Tester, J.W., 2016. Uncertainty analysis of geothermal well drilling and completion costs. Geothermics 64, 382–391. https://doi.org/10.1016/j.geothermics.2016.06.017

Lund, J.., 2001. Geothermal Heat Pumps - An overview. GHC Bull. 22, 1–8.

Malolepszy, Z., 2003. Man-made, low-temprature reservoirs in abandoned workings of underground mines on example of Nowa Ruda coal mine, Poland, in: International Geothermal Conference. Reykjavík, pp. 23–29.

Malolepszy, Z., Demollin-Schneiders, E., Bowers, D., 2005. Potential Use of Geothermal Mine Waters in Europe, in: Proceedings World Geothermal Congress. Antalya, Turkey, pp. 24–29.

Marino, G.G., Gamble, W., 1986. Mine subsidence damage from room and pillar mining in Illinois. Int. J. Min. Geol. Eng. 4, 129–150.

Martin, C.D., Maybee, W.G., 2000. The strength of hard-rock pillars. Int. J. Rock Mech. Min. Sci. 37, 1239–1246. https://doi.org/10.1016/S1365-1609(00)00032-0

McCay, A.T., Shipton, Z.K., Lunn, R.J., Gale, J.F., 2019. Mini thief zones: Subcentimeter sedimentary features enhance fracture connectivity in shales. Am. Assoc. Pet. Geol. Bull. 103, 951–971. https://doi.org/10.1306/0918181610617114

Mcmechan, G.A., Loucks, R.G., Mescher, P., Zeng, X., 2002. Characterization of a coalesced , collapsed paleocave reservoir analog using GPR and well-core data 67, 1148–1158.

Menéndez, J., Ordóñez, A., Álvarez, R., Loredo, J., 2019. Energy from closed mines: Underground energy storage and geothermal applications. Renew. Sustain. Energy Rev. 108, 498–512. https://doi.org/10.1016/j.rser.2019.04.007

Monaghan, A.A., Dochartaigh, B.O., Fordyce, F., Loveless, S., Entwisle, D., Quinn, M., Smith, K., Ellen, R., Arkley, S., Kearsey, T., Campbell, S.D.., Fellgett, M., Mosca, I., 2017. UKGEOS - Glasgow Geothermal Energy Research Field Site (GGERFS): Initial summary of the geological platform. Br. Geol. Surv. Open Rep. OR/17/006, 205.

Moore, D.G., 1961. Submarine Slumps. J. Sediment. Res. 31, 343–357. https://doi.org/10.1306/74d70b78-2b21-11d7-8648000102c1865d

Murchison, D., Pearson, J., 2000. The anomalous behaviour of properties of seams at the Plessey (M) horizon of the Northumberland and Durham coalfields 79, 865–871.

Nef, J.., 1965. The Rise of the British Coal Industry, 2nd ed, The British Journal of Psychiatry. Frank Cass & Co. Ltd., Abingdon. https://doi.org/10.1192/bjp.111.479.1009-a

Page, W., 1907. The Victora History of the Counties of England: A History of Durham (Volume 2), Vol 2. ed. Archibald Constable and company limited, London, UK.

Patsa, L., Zarrouk, S.J., Patsa, E., Van Zyl, D., Arianpoo, N., 2015. Geothermal Energy in Mining Developments: Synergies and Opportunities Throughout a Mine’s Operational Life Cycle, Proceedings World Geothermal Congress.

Poulsen, B.A., Shen, B., 2013. Subsidence risk assessment of decommissioned bord-and-pillar collieries. Int. J. Rock Mech. Min. Sci. 60, 312–320. https://doi.org/10.1016/j.ijrmms.2013.01.014

Salmi, E F, Karakus, M., Nazem, M., 2019. Assessing the e ff ects of rock mass gradual deterioration on the long-term stability of abandoned mine workings and the mechanisms of post-mining subsidence – A case study of Castle Fields mine. Tunn. Undergr. Sp. Technol. 88, 169–185. https://doi.org/10.1016/j.tust.2019.03.007

Salmi, Ebrahim F, Malinowska, A., Hejmanowski, R., 2019. Investigating the post-mining subsidence and the long-term stability of old mining excavations : case of Cow Pasture Limestone Mine , West Midlands, UK. Bull. Eng. Geol. Environ. 1–18.

Sanner, B., 2001. Shallow Geothermal Energy. GHC Bull. June.

Smailes, A.E., 1938. Population Changes in the Colliery Districts of Northumberland and Durham. Geogr. J. 91, 220. https://doi.org/10.2307/1787541

Smails, A.E., 1935. The development of the Northumberland and Durham coalfield. Scott. Geogr. Mag. 51, 201–214. https://doi.org/10.1080/14702543508554344

Soper, N.J., Webb, B.C., Woodcock, N.H., 1987. Late Caledonian (Acadian) transpression in north-west England:

timing, geometry and geotectonic significance. Proc. Yorksh. Geol. Soc. 46, 175–192.

Stumm, W., Morgan, J.J., 1981. Aquatic chemistry: an introduction emphasizing chemical equilibria in natural waters. John Wiley & Sons, Hoboken, NJ.

Tingay, J., Ellis, M., 2016. Hartley Cove to the River Tyne Coastal Strategy Coastal Processes Quality Management Quality Management. North Tyneside.

Turner, B.R., Richardson, D., 2004. Geological controls on the sulphur content of coal seams in the Northumberland Coalfield, Northeast England. Int. J. Coal Geol. 60, 169–196. https://doi.org/10.1016/j.coal.2004.05.003

Wardell, K., Wood, J.C., 1965. Ground instability problems araising from the presence of shallow old mine workings. Proc. Midl. Soc. Soil Mech. Found. Eng. 7, 7–30.

Warren, J.K., 2016. Hypersaline Fluid Evolution During Burial and Uplift, in: Evaporites. Springer International Publishing, pp. 763–832. https://doi.org/10.1007/978-3-319-13512-0_8

Woodcock, N.H., Mort, K., 2008. Classification of fault breccias and related fault rocks. Geol. Mag. 145, 435–440. https://doi.org/10.1017/S0016756808004883

Younger, P.L., 2004. Environmental impacts of coal mining and associated wastes: A geochemical perspective. Geol. Soc. Spec. Publ. https://doi.org/10.1144/GSL.SP.2004.236.01.12

Younger, P.L., 1998. Coalfield abandonment: geochemical processes and hydrochemical products., in: Nicholson, K. (Ed.), Energy and the Environment-Geochemistry of Fossil, and Renewable Resources. Environmental Geochemistry Series No. 1, Aberdeen (UK), p. 200.

Younger, P.L., 1995. Hydrogeochemistry of minewaters flowing from abandoned coal workings in County Durham The Durham minewater study Scope of the study. Q. J. Eng. Geol. Hydrogeol. 28, S101–S113.

Younger, P.L., 1994. Minewater pollution; the revenge of Old King Coal. geoscientist 4, 6–8.

Younger, P.L., Banwart, S.A., Hedin, R.S., 2002. Mine water: hydrology, pollution, remediation, Vol. 5. ed. Springer Science & Business Media.